CHANNEL FLOW LES WITH SPECTRAL ELEMENTS

Hugh M. Blackburn

Division of Building, Construction and Engineering
CSIRO, Highett, Victoria, AUSTRALIA

Department of Mechanical Engineering
Monash University, Clayton, Victoria, AUSTRALIA

ABSTRACT

Results from spectral element large eddy simulations of turbulent channel flow are presented. A Smagorinsky subgrid-scale stress model was employed, and van Driest-type wall damping was needed, as is usually the case for wall-resolving large eddy simulations with the Smagorinsky model. Simulation results compare favorably with experimental measurements at the same Reynolds number, demonstrating the potential of the method in wall-bounded flows of higher geometric complexity.

INTRODUCTION

Spectral element spatial discretisations hold promise for large eddy simulation (LES) of turbulent flows in complex geometries. This prospect results from the combination of the ability to provide arbitrary geometric complexity and high accuracy with low numerical diffusion and dissipation. Despite this, spectral element methods have not yet been widely employed for LES.

The current work documents results from spectral element channel flow LES with a Smagorinsky subgrid-scale stress (SGSS) model. Turbulent channel flow has been extensively investigated both experimentally and numerically, and serves here as a prototype wall-bounded flow for spectral element LES, in a simple geometry.

Based on the wall friction velocity $u_\tau = (\tau_w/\rho)^{1/2}$ and the channel semi-width δ, the Reynolds number used in the simulation was $Re_\tau = u_\tau \delta/\nu = 651$. This corresponds approximately to results presented by Hussain & Reynolds (1975), with the centreline Reynolds number $Re_c = U_c \delta/\nu = 13\,800$, where U_c is the mean centreline flow speed.

LES METHODOLOGY

The principle underlying LES is that a resolved scale (explicitly represented) field $\overline{u}$ is obtained from the underlying complete turbulent field u by convolution with a filter function K,

$$\overline{u}(r) = \int K(\Delta, |r - r'|)\, u(r')\, \mathrm{d}^3 r'. \qquad (1)$$

The filtering operation is implicit in the formulation (i.e. not explicitly carried out). Under assumptions which are generally non-restrictive (see e.g. Leonard 1974), filtering and differentiation commute, i.e. $\overline{\partial u/\partial x} = \partial \overline{u}/\partial x$.

Filtering the incompressible Navier–Stokes equations leads to

$$\frac{\partial \overline{u}}{\partial t} + \nabla \cdot \overline{uu} = -\nabla \overline{P} + \nu \nabla^2 \overline{u}, \qquad (2)$$

where $P = p/\rho$. As in conventional turbulence modelling, the nonlinear terms are not closed, because the filtered dyad $\overline{uu}$ is not available in terms of the resolved components $\overline{u}$. To overcome the problem, the concept of a subgrid-scale stress τ is introduced, such that $\overline{uu} = \overline{u}\,\overline{u} + \tau$. Then the momentum equation becomes

$$\frac{\partial \overline{u}}{\partial t} + \nabla \cdot \overline{u}\,\overline{u} = -\nabla \overline{P} + \nu \nabla^2 \overline{u} - \nabla \cdot \tau, \qquad (3)$$

and the turbulence modelling task is to predict the subgrid-scale stress τ from the resolved velocity field u.

SGSS model

This investigation of the use of spectral elements for LES has employed an eddy-viscosity SGSS model. This assumes that the anisotropic part of τ is related to the resolved strain rate field through a scalar eddy viscosity,

$$\tau - \frac{1}{3}\operatorname{tr}(\tau)1 = -2\nu_t \overline{S} = -\nu_t \left[\nabla \overline{u} + (\nabla \overline{u})^t \right], \quad (4)$$

with the isotropic part of τ subsumed in P.

The Smagorinsky (mixing length) model is used to obtain the turbulent eddy viscosity from the strain rate magnitude,

$$\nu_t = (C_S \Delta)^2 2^{1/2} |S| = (C_S \Delta)^2 \operatorname{tr}(2\overline{S}^2)^{1/2}, \qquad (5)$$
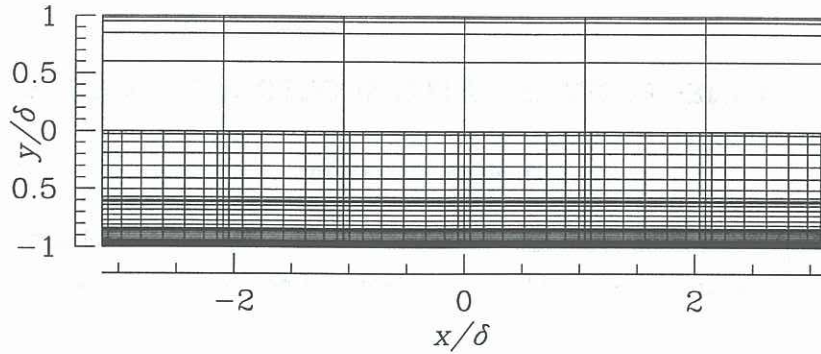
989

Figure 1: Two-dimensional section of 60-element mesh. The upper half of the mesh shows spectral element boundaries, the lower half shows the element nodes for 8×8 tensor-product shape functions.

where C_S is a model constant and $\Delta = (\Delta x \Delta y \Delta z)^{1/3}$ is a measure of the local grid length scale.

Wall treatment

Rather than use a wall-function approach to the treatment of solid boundaries, the near-wall regions of the flow are resolved. It is known that in this case, the Smagorinsky treatment of the eddy-viscosity must be modified using a van Driest-type wall damping, which switches off the turbulence model in the near-wall region.

A form which gives the correct near-wall asymptotic behaviour of SGSS is that introduced by Piomelli, Ferziger & Moin (1987), where the turbulent mixing length $C_S \Delta$ is modified as

$$C_S \Delta \left[1 - \exp(-(y^+/A^+)^3) \right]^{1/2}, \qquad (6)$$

with y^+ as the dimensionless wall-normal distance $y/(u_\tau/\nu)$ and the constant $A^+ = 26$. The damping only has significant effect for $y^+ < 40$. Note that this approach requires that the mean wall shear stress be known in order to determine $y = y^+ u_\tau / \nu$. This does not present a problem in the present application, as the time-mean wall shear stress is specified. In a more general case, this approach would be more difficult to implement as u_τ would not be known in advance.

NUMERICAL TECHNIQUE

The spatial discretisation employs a spectral element/Fourier formulation, which allows arbitrary geometry in the (x, y) plane, but requires periodicity in the z (out-of-plane) direction. The basis of the method as applied to DNS of the incompressible Navier–Stokes equations has been described by Karniadakis & Henderson (1998). The nonlinear terms of (3) have been implemented here in skew-symmetric form, i.e. $(\overline{u} \cdot \nabla \overline{u} + \nabla \overline{u}\, \overline{u})/2$, because this has been found to reduce aliasing errors.

The method requires some slight modification in order to deal with the $\nabla \cdot \tau$ terms in (3). The ap-

proach taken here follows that outlined in Karnidakis, Orszag & Yakhot (1993), in that the sum of the molecular and turbulent eddy viscosities $\nu_T = \nu_t + \nu$ is decomposed into a spatially-constant component λ and a spatially-varying component ϵ. This allows integration of the ϵ-contribution to $-\nabla \cdot \tau$, i.e. $\nabla \cdot \epsilon \left[\nabla \overline{u} + (\nabla \overline{u})^t \right]$, to be dealt with explicitly, while the remainder is dealt with implicitly through the operation $\lambda \nabla^2 \overline{u}$, thus enhancing the overall numerical stability of the scheme.

In order to use a domain with periodicity in the streamwise (x) as well as spanwise (z) directions, a body force per unit mass of magnitude $\tau_w / \rho \delta$ was applied to the x-component of (3). This approach allows the pressure to be periodic in the streamwise direction.

As a result of the Fourier decomposition, implementation of the time integration as a parallel algorithm is straight-forward, with inter-process communication required only during formulation of the nonlinear terms in (3). The message-passing kernel MPI has been used for this operation, and the computations reported here were carried out using four processors on an NEC SX-4 computer.

Mesh parameters

The computational mesh is chosen first on the basis that the size of the domain represented is 'sufficiently large', with the mesh spacing decided by resolution requirements.

In the channel-flow geometry, which formally is infinite in two spatial directions, the spanwise and streamwise modules are usually based on the respective integral correlation lengths of turbulence, as obtained in physical experiments. The lengths often used (see e.g. Moin, Reynolds & Ferziger 1978) are $L_x = 2\pi\delta$ in the streamwise direction and $L_z = \pi\delta$ in the spanwise direction, and these have been adopted here.

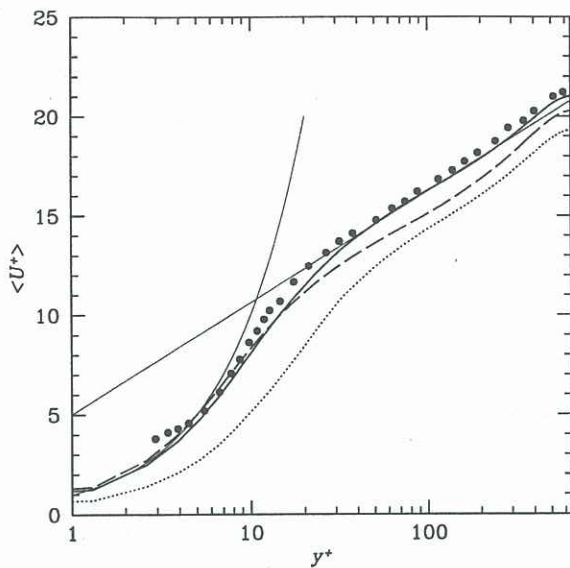Another important consideration is resolution near

Figure 2: Mean velocity profiles. •, $Re_c = 13\,800$ experimental results of Hussain & Reynolds (1975); ——, Law of the Wall; − −, No model; ·····, Smagorinsky model, no wall damping; ——, Smagorinsky model with wall damping of Piomelli et al. (1987).

Figure 3: Resolved scale fluctuating streamwise velocity. •, $Re_c = 13\,800$ experimental results of Hussain & Reynolds (1975); ——, LES results.

the wall. According to the recommendations of Piomelli (1997) for wall-resolving LES, the first mesh point away from the wall should be located at $y^+ < 1$, and $\Delta x^+ \simeq 50$–100, $\Delta z^+ \simeq 15$–40. Using 10 spectral elements in the wall-normal direction and a geometric progression of sizes leads to 8×8 tensor-product shape functions for $y^+ = 1$ at the first node point. Choosing 6 elements in the x-direction and 64 planes of data in the z-direction provides $\Delta x^+ \approx 85$, $\Delta z^+ \approx 30$. The corresponding two-dimensional mesh is shown in figure 1. There are just less than $250\,000$ mesh points for the three-dimensional domain.

The Smagorinsky constant $C_S = 0.065$, in line with previous channel flow LES experience. The local mesh lengths Δx, Δy used to compute Δ were evaluated by dividing the local element lengths by the order of the tensor-product shape functions, i.e. $(np - 1)$ where np is the number of mesh points along an element edge. $\Delta z = \pi/64 = 0.049$.

RESULTS
Mean velocity
Mean velocity profiles are displayed in figure 2 in wall units: $U^+ = u/u_\tau$, $y^+ = y u_\tau/\nu$. For comparison purposes the $Re_c = 13\,800$, $Re_\tau = 640$ experimental results of Hussain & Reynolds (1975) are shown, along with a 'Law of the Wall' plot which uses $U^+ = 5 + 2.44 \ln y^+$ in the logarithmic region.

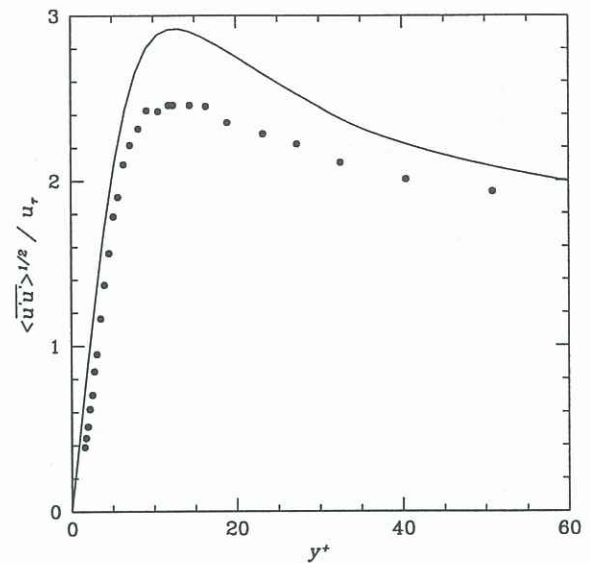It can be seen that the model parameters provide a

satisfactory match between the computed and experimental results. The agreement is least satisfactory in the buffer layer, i.e. $5 < y^+ < 35$, where most turbulent energy production occurs. The poor agreement near the wall ($y^+ < 5$) is due to resolution problems in the experiment.

In order to examine the individual contributions of the turbulence model, two other sets of results are also presented in figure 2. The first is the 'no model' case, i.e. a direct numerical simulation on the same mesh. As expected, this shows good agreement with the Law of the Wall in the linear sublayer region ($y^+ < 5$), but exhibits less good agreement in the outer region. The importance of the wall damping model can be seen from the remaining set of results, for which the Smagorinsky model is used without modification right down to the wall. It can be seen that this results in very poor agreement in the near-wall region, contaminating the entire simulation. The effect of the wall damping (6) is to switch off the turbulence model in the near-wall region, which leads to the similarity of the no-model and full-model LES results there.

Fluctuating velocity
The resolved-scale streamwise standard deviation velocity profile from the LES results is shown in figure 3; again, results from Hussain & Reynolds (1975) are shown for comparison. It can be seen while the peak of the profile occurs at approximately the correct distance from the wall ($y^+ \approx 15$, in the buffer region), the fluctuating velocities are higher than the experimental results of Hussain & Reynolds. Similar be-
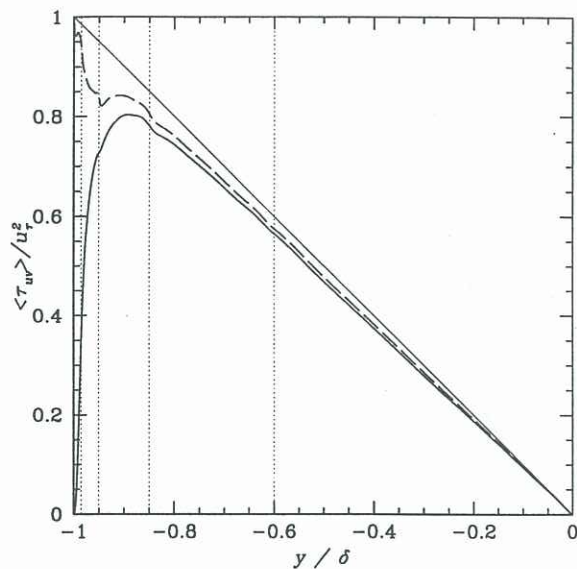
Figure 4: Resolved scale shear stress. ——, Resolved scale Reynolds stress; − −, Resolved scale Reynolds stress plus viscous stress; ——, Total mean shear stress; ⋯⋯, Element boundary levels.

haviour can be seen for example in the wall-resolving LES results of Piomelli et al. (1987).

Shear stress

Figure 4 shows the mean resolved-scale shear stress profile. Note the lines showing the element-boundary elevations. As we move to higher-order statistics the influence of the underlying spectral element discretisation becomes more apparent—here it can be inferred that the subgrid-scale component of the shear stress (the difference between the total and the Reynolds plus viscous contribution) tends to peak along element boundary locations. This is largely due to the use of element-wise collocation derivatives in computing terms for the SGSS model.

DISCUSSION

With spectral element mesh parameters that are broadly in line with established practice for channel flow LES, and the simplest available SGSS model, we have obtained results that agree well with turbulent channel flow experiments and also with previous LES results. The emphasis has been on demonstrating that the spectral element technique can be used for LES, rather than the flexibility of the discretisation. For example, even within this simple geometry, significant savings in the number of mesh points could be achieved by employing a hierarchical refinement of element sizes as we move towards the wall, using either conforming or non-conforming element connectivities.

In order to move to arbitrarily-complex geometries, SGSS models and wall treatments that do not rely on prior knowledge of the wall shear stress distribution are required. In this area, the adoption of either dynamic or recent scale-similarity models holds promise. A further requirement will be the development of element-wise operations that tend to minimise aliasing problems in the production of high order nonlinear terms.

CONCLUSIONS

The present results demonstrate that spectral element techniques can be employed for LES with reasonable success, and results are similar to those obtained with other discretisation schemes. The chosen geometry does not exploit the geometric flexibility of the method, and this will be one goal of future work. Another will be to adopt SGSS models and wall treatments that do not depend on *a priori* knowledge of wall shear stresses.

REFERENCES

HUSSAIN, A. K. M. F. & REYNOLDS, W. C. (1975). Measurements in fully-developed turbulent channel flow, *ASME J. Fluid Engng* **97**: 568–578.

KARNIADAKIS, G. E. & HENDERSON, R. D. (1998). Spectral element methods for incompressible flows, *in* R. W. Johnson (ed.), *Handbook of Fluid Dynamics*, CRC Press, Boca Raton, chapter 29, pp. 29–1–29–41.

KARNIADAKIS, G. E., ORSZAG, S. A. & YAKHOT, V. (1993). Renormalization group theory simulation of transitional and turbulent flow over a backward-facing step, *in* B. Galperin & S. A. Orszag (eds), *Large Eddy Simulation of Complex Engineering and Geophysical Flows*, Cambridge, chapter 8, pp. 159–177.

LEONARD, A. (1974). Energy cascade in large-eddy simulations of turbulent fluid flows, *Adv. Geophys.* **18A**: 237–248.

MOIN, P., REYNOLDS, W. C. & FERZIGER, J. H. (1978). Large eddy simulation of incompressible turbulent channel flow, *Technical Report TF-12*, Department of Mechanical Engineering, Stanford University.

PIOMELLI, U. (1997). Large-eddy simulations: Where we stand, *in* C. Liu & Z. Liu (eds), *Advances in DNS/LES*, AFOSR, Louisiana, pp. 93–104.

PIOMELLI, U., FERZIGER, J. H. & MOIN, P. (1987). Models for large eddy simulations of turbulent channel flows including transpiration, *Technical Report TF-32*, Department of Mechanical Engineering, Stanford University.